1 Review of the CO Oxidation on Pt*

> *"The experiments seem to indicate that nearly but not quite all the reaction take place between oxygen atoms adsorbed on the surface and carbon monoxide molecules from the gas phase which strike them".*
> *…" We might expect the flanks of an adsorbed (oxygen) film to be more susceptible to chemical action"… . In this case the oxygen film would be removed progressively from its bounding edge inward".*
> *"Carbon monoxide has a …(poisoning), but more transient effect on platinum, for only as long as this gas remains present in the gas phase does the poisoning influence persist ".*
>
> I. Langmuir, Ibidem

A consistent part of the automotive processes involve the CO oxidation on supported metal catalysts [1]. The materials used in the practical applications are the so-called *three-way* composite catalysts such as $Pt/Rh/Ce0_2/Al_2O_3$, capable of oxidizing CO and hydrocarbons (HC) and reducing nitrogen oxides (NO_x) at the same time [2].

The kinetics of this reaction has been extensively studied. Isothermal temporal oscillations in the CO-oxidation rate were discovered by P. Hugo [3] and M. Jakubith [4] in 1970 on a platinum contact. Similar phenomena on Pt single-crystal surfaces were found by G. Ertl and coworkers on Pt(100) in 1982 [5] and M. Eiswirth and G. Ertl on Pt(110) in 1986 [6]. M.P. Cox and co-workers found a correlation between temporal oscillations and surface structure [7] and by using a scanning-LEED technique were able to observe spatio-temporal patterns [8]. Models of the reaction were implemented to describe temporal [9] and spatio-temporal [10] self-organization patterns arising due to the nonlinear character of this open, *far-from-equilibrium* system. With the development of dedicated imaging methods (PEEM [11] and EMSI [12] are both described in the next chapter), it became possible to investigate the structures arising from the lateral variations of the concentration of the species at the surface [13].

* References at page 14

In the following, the main features of the CO oxidation on platinum (110) are summarized, starting with the description of the single crystal platinum surface, and the characteristics of oxygen and carbon monoxide adsorption on Pt(110) (see also reference [14]). The coadsorption of both species and the mechanism of the reaction are presented, together with nonlinear effects such as reaction rate oscillations and concentration pattern formation.

1.1 The platinum (110) surface

At room temperature the clean (110) surface of a fcc platinum crystal (a = 3.92 Å) (Fig. 1.1) displays a different structure than the corresponding bulk planes. The LEED pattern shows a (1x2) reconstruction [15], commonly explained in terms of the *missing row* model [16] (Fig. 1.2): every second $[1\bar{1}0]$ close-packed row is absent. The driving force for this rearrangement is the lowering of the surface energy upon the formation of (111) nanofacets.

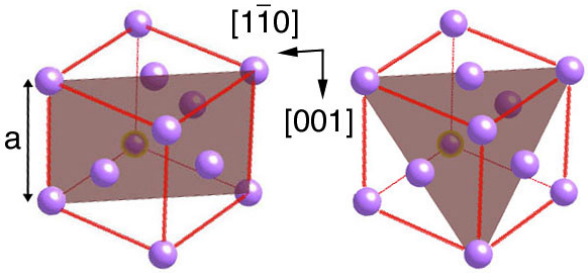

Fig.1.1 The (110) and (111) surfaces of a fcc crystal.

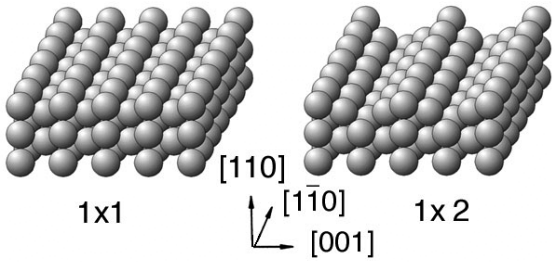

Fig. 1.2 The Pt(110) (1x1) and (1x2) surfaces.

The mechanism of the surface transformation is discussed in Sect. 1.4, after a presentation of the characteristics of oxygen and carbon monoxide adsorption on Pt(110) in Sect. 1.2 and. 1.3, respectively.

1.2 Carbon monoxide adsorption on Pt(110)

"The carbon atom (in the CO molecule is) directly combined with the platinum"
I. Langmuir, Ibidem.

While the CO adsorption on reactive surfaces such as alkali and rare earth metals is normally dissociative [1], on d-metal surfaces (e.g. Cu, Ag) it is predominantly molecular, and the strength of the CO–metal bond is relatively weak. In fact, by increasing the temperature of the substrate CO desorbs molecularly before dissociatiating. For the majority of the transition metals, however, the nature of the adsorption is very sensitive to the temperature and the structure of the surface.

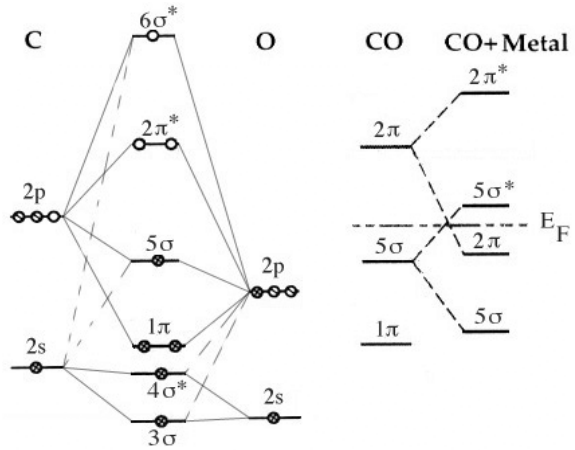

Fig. 1.3 MO diagram for a CO–metal system.

On the Pt(110) surface CO adsorbs in a molecular form. The CO bonding on Pt as well as on other transition metal surfaces is explained by the Blyholder model [17], originally developed for metal carbonyl systems [18]. The 5σ and the 2π frontier molecular orbitals (MO) of the CO molecule are substantially modified by the presence of the metal surface (Fig.1.3, after [19]). A filled 5σ "lone pair" orbital interacts with the empty dσ metal orbitals, leading to a partial transfer of electron density to the metal. At the same time the filled metal dπ orbitals overlap with the 2π* antibonding molecular orbital of the CO (Fig. 1.4).

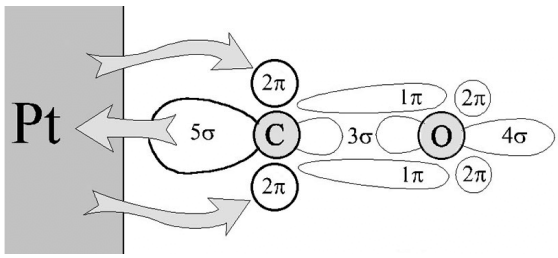

Fig. 1.4 The donation-backdonation mechanism.

Since in the course of this electron donation-backdonation process anti-bonding orbitals are populated, the strength of the carbon–oxygen bond [20] and, as a consequence, the stretching frequency [21] are lowered, compared to the isolated molecule in the gas phase. Moreover, since the 5σ and 2π MO of CO are localized mainly at the C atom, the bonding occurs with the carbon atom facing the surface.

Dosing more than 1 L CO on a Pt(110) surface at temperatures between 250 and 500 K results in a (1x1) LEED pattern exhibiting a high degree of disorder. As discussed later in Sect 1.5, at a coverage of 0.2 [15] CO starts lifting the (1x2) surface reconstruction [22]. An ordered (2x1)p2mg CO overlayer, at $\Theta \approx 1$, is only achieved by cooling down the crystal from 500 K in a CO atmosphere at 10^{-7} mbar. At all coverages predominantly on-top sites are populated [23], and the growth proceeds via island formation [24]. The diffusion coefficient of CO along the [1$\bar{1}$0] axis is $5.5 \cdot 10^{-8}$ cm$^2 \cdot$ s^{-1} at 438 K, twice as large as the one in the perpendicular [001] direction [25].

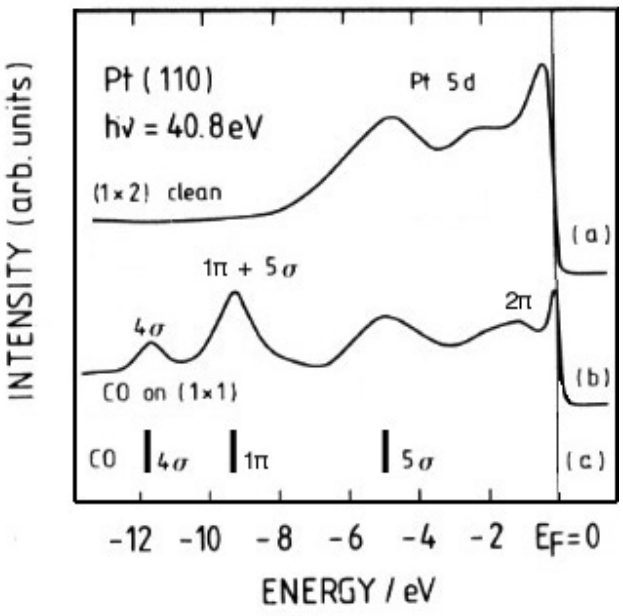

Fig. 1.5 UPS of a): Pt(110); b) CO/Pt(110); c) CO in the gas phase.

UPS data [26], shown Fig. 1.5, reveal the presence of the 4σ and 1π MO of adsorbed CO, the shift of the 5σ and 2π compared to the isolated molecule, and marked decrease of the electron density of states in the metal close to the Fermi level. The distribution of the density of electron states near the Fermi edge are considered later in Chap. 3, where TDS and work-function investigations are presented.

1.3 Oxygen on Pt(110)

On a Pt(110) surface oxygen adsorbs molecularly at T < 120 K and dissociatively at higher temperature [27]. At 300 K oxygen adsorbs initially on the 4-fold coordinated sites located at the bottom of the [1$\bar{1}$0] valleys [28]. At higher exposures even the 3-fold (111) nanofacets, in Fig. 1.6 after [29], start to be populated. Other authors instead favor, the occupation of the site at the walls of the troughs [30]. The saturation coverage at 300 K is estimated to be 0.35 ML [26], in agreement with the recent results of Walker et al. [30]. In the latter article the authors also report a value of 0.4 for the initial sticking coefficient at 300 K.

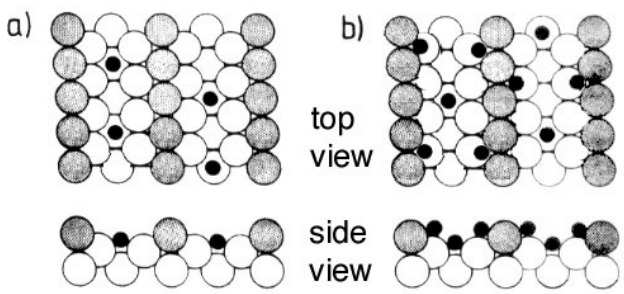

Fig. 1.6 O/ Pt(110): a) low and b) high coverage.

Fig. 1.7 TD data of O_2/Pt(110)

At about 800 K recombinative molecular desorption takes place (see Fig. 1.7 after [31]).The dissociation of oxygen on metal surfaces has been modeled by ab-initio fully quantum-dynamical simulations [28] [32]. The role of the electronic energy states in the dissociative adsorption of O_2 has been studied by Heiz and coworkers [33] by varying the size of Pt clusters, and, in turn, the position of the d-band. They found that oxygen dissociation occurs preferentially on those clusters whose states induce enough backdonation into the antibonding $2\pi_g^*$ state or a sufficient donation from the $1\pi_u$ or $5\sigma_g$ oxygen molecular orbitals into the cluster. Both processes, in fact, reduce the bond order of the oxygen molecule. On the Pt(110) surface oxygen atoms diffuse preferentially along the $[1\bar{1}0]$ direction [25]. The macroscopic diffusion coefficient, strongly dependent on the oxygen coverage, is on the order of 10^{-8} $cm^2 \cdot s^{-1}$ at 600 K.

Since O atoms diffuse relatively easily into the bulk of metals, a number of different, not always well defined, chemisorbed, surface oxide, subsurface, and oxide species have been reported. It is beyond the scope of this thesis to discuss any details of this subject [34] [35] [36] [37]. However, results reproducing a key experiment on subsurface oxygen [38] are presented in chapter 4.

1.4 Surface reconstruction mechanism

Two different phases of the Pt(110) surface can be observed, depending on the preparation procedure. Right after Ar ions sputtering a metastable (1x1), disordered structure can be observed, which converts within a short time into the (1x2) structure. An adsorbate-induced lifting of the (1x2) surface reconstruction occurs upon CO adsorption, starting at a CO coverage of 0.2 ML. Moreover, under appropriate reaction conditions, a faceting of the Pt(110) surface is reported at temperature below 500 K [39]. These facets consist of steps and terraces in the [001] direction with a spatial periodicity on the order of 100 Å. The (1x2) is destabilized above 900 K, as displayed by a blurry (1x1) LEED pattern [40].

It is notable that in order to transform the ordered missing row into an ideal bulk-terminated structure (Fig. 1.2), an extensive mass transport, involving a substantial rearrangement of a large part of the surface Pt atoms, is needed. The key point for the interpretation is that the diffraction pattern [23] of the *deconstructed* [41] CO/Pt(110) (1x1) surface does not correspond to an ordered structure but rather to a strongly disordered system. A similar behavior was found for NO/Pt(110) [42].

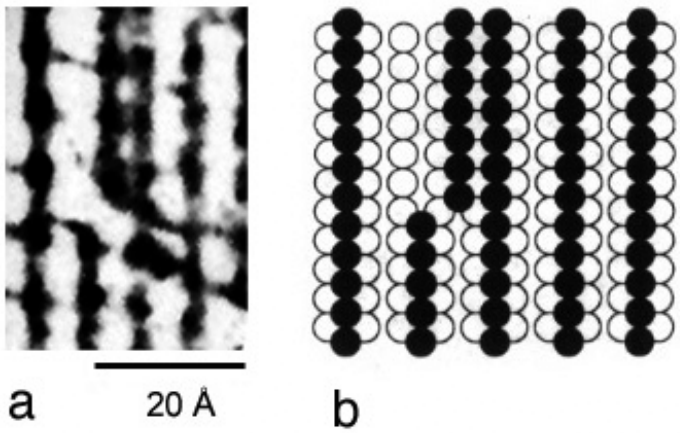

Fig. 1.8 The *row pairing* mechanism; a: an STM image; b: a schematic model.

It was observed (Fig. 1.8a after [43]) that the transition occurs locally by displacing single Pt atoms from (1x2) sites. Therefore, in what appears as an order-disorder transition, Pt atoms of the first layer begin to diffuse out of the $[1\bar{1}0]$ rows and occupy lattice sites without (1x2) periodicity. At high CO coverages the atoms are randomly distributed on all possible lattice sites determined by the bulk. At this point the diffraction pattern is indistinguishable from the one of a perfectly ordered (1x1) surface. As a result, additional sites in the second platinum atomic layer start to be accessible for the adsorption, which accounts for the increased oxygen sticking probability on the (1x1) surface.

Why should the Pt atoms involved in a bond with the adsorbed CO move laterally? Some hints come from a study of CO on Ru/SiO_2 [44]. The adsorption of CO has been noticed to cause disruptions of Ru–Ru bonds in the metal clusters and the formation of a mobile Ru–CO species. Although it is evident that energy minimization represents the driving force for the adsorbate-induced reconstruction, a complete understanding of the phenomenon seems still to be lacking.

1.5 O_2 and CO on Pt(110): the reaction

It is now widely accepted that the reaction proceeds via the Langmuir-Hinshelwood mechanism [45]. Both reactants adsorb on the catalyst surface in order to yield the product. The reaction centers of the metal are the coordination-unsaturated surface atoms with underpopulated d orbitals. The reaction steps are:

$$CO(g) + \otimes \leftrightarrow CO_{AD}$$
$$O_2(g) + \otimes\text{-}\otimes \rightarrow 2O_{AD}$$
$$CO_{AD} + O_{AD} \rightarrow CO_2(g) + \otimes\text{-}\otimes.$$

They correspond to the molecular and dissociative adsorption of CO and O_2, respectively, and the subsequent diffusion of a CO towards an oxygen atom, followed by the production of CO_2, which immediately leaves the surface. Since oxygen needs two adjacent free sites (indicated with ⊗-⊗) for the chemisorption, the coadsorption characteristics of the two species are quite different, depending on the sequence of the adsorption: a phenomenon named *asymmetric inhibition* (Fig. 1.9). While at all oxygen coverages there is still enough place to accommodate CO molecules, oxygen adsorption is completely blocked by carbon monoxide already at a coverage of 0.3 ML due to the lack of available pairs of neighbor sites. The observed [27] increase of the oxygen sticking probability on the (1x1) surface looks puzzling, since the CO at the concentration required to lift the reconstruction is expected to inhibit any oxygen adsorption.

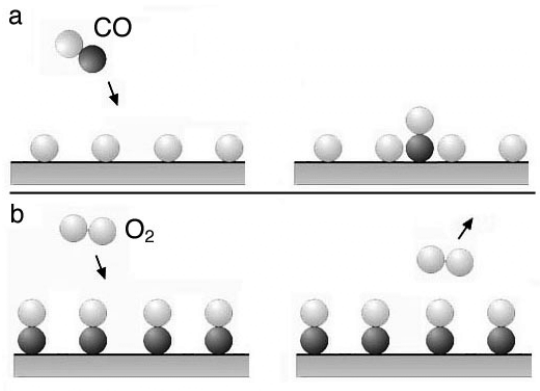

Fig. 1.9 The asymmetric inhibition. a: CO adsorption on a oxygen precovered surface; b: O_2 adsorption on a CO predosed surface.

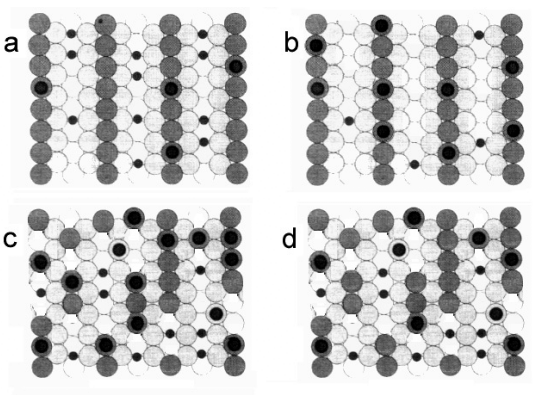

Fig. 1.10 Schematic of the reaction cycle.

Fig. 1.10a shows how on a prevalently O covered surface the CO adsorbs and reacts easily forming CO_2, consuming the oxygen (b), until the critical coverage necessary to lift the reconstruction is reached (c). New highly coordinated empty sites, created in the course of the process, favor oxygen adsorption and reaction, consuming CO. The CO concentration falls (d), restarting the cycle.

An increase of the catalytic activity, interpreted as an increased oxygen sticking probability, was observed in correlation with the process of faceting of the surface during the reaction at temperature between 400 and 500 K [39]. In such cases, instead of oscillations, a continuous rise of the CO_2 production rate has been observed.

1.6 Reaction modeling

Ab-initio density functional theory has been employed to simulate the reaction pathway for small systems consisting typically of few Pt, O, and C atoms (e.g. on Pt(111) [46]). All the important structural parameters can be obtained by optimization [47], allowing even to draw conclusion about the short-range nature of the adsorbate–metal bonding. Recent calculations [48] revealed that a favorable reaction pathway proceeds by CO diffusion towards a neighboring O atom. This causes a notable weakening of the O–metal bond strength apparently due to competition for the bonding charge of the metal atoms, enabling the O atom to react with the CO molecule.

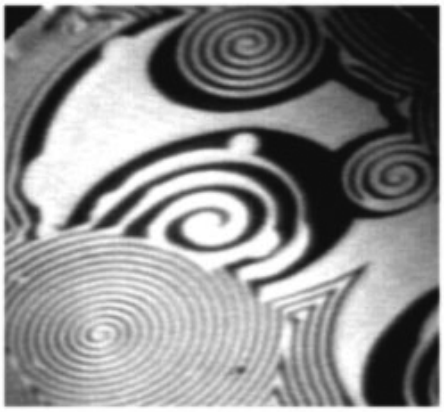

Fig. 1.11 Concentration pattern in the CO-oxidation on Pt(110).

The evolution of the adlayer as a whole and the formation of patterns in the CO oxidation on platinum (Fig. 1.11 after [49]) can be modeled mathematically by means of different techniques according to the type of approximation. On a microscopic level, the *master equation* [50] deals with an ensemble of individual lattice sites, their occupation and the *transition* probabilities among them. The dynamics is inherently driven by internal (in the transitions) as well as external (as in the temperature) fluctuations. Due to the complexity of the system, *realizations* (an expression for *solutions* in this context) of the microscopic dynamics are typically obtained by applying Monte-Carlo methods. In the *Fokker-Planck* approach [51] some spatial average is applied and only *weak* noise is considered. In the automaton model [52], on the contrary, an artificial dynamics, mimicking the essential features of the real reactive dynamics, which is simple enough to permit efficient simulation, is tailored. If properly constructed, this mesoscopic dynamics yields the reaction-diffusion equations and incorporates effects of molecular fluctuations.

The mesoscopic characteristic length of spatial pattern in the CO oxidation have been successfully reproduced [9], [53] within the *mean-field reaction-diffusion equation* [54] analyses, in which no fluctuation and only global properties are considered.

The following set of three coupled non-linear partial differential equations describes the rate of CO and oxygen coverage and the portion of (1x1) surface, u, v, and w, respectively:

$$\frac{\partial u}{\partial t} = k_1 p_{CO}\left(1-u^3\right) - k_2\, u - k_3\, u\, v + D_{xx}\frac{\partial^2 u}{\partial x^2} + D_{yy}\frac{\partial^2 u}{\partial y^2}$$
$$\frac{\partial v}{\partial t} = k_4\, p_{O_2}\left[s_{O,1x1} w + s_{O,1x2}(1-w)\right](1-u-v)^2 - k_3\, u\, v$$
$$\frac{\partial w}{\partial t} = k_5\left[f(u) - w\right].$$

The terms in the first equation describe the CO precursor adsorption, desorption, reaction, and diffusion. The latter accounts for the spatial coupling in the reaction. Thanks to the *Onsager's reciprocity relations* [55] the diffusion constant **D**, in general a 2-dimensional tensor, can always be diagonalized ($\mathbf{D} = \delta_{ij} \cdot D_{ij}$). The effects of the asymmetrical inhibition and of the oxygen sticking coefficient dependence on the surface geometry are taken into account in the second equation. Oxygen diffusion, negligible compared to CO, is not considered. The third equation contains a function f(u) of the carbon monoxide concentration mimicking the empirical data of adsorbate-induced surface reconstruction. In the framework of the mean-field approximation the CO adsorption-desorption kinetic is studied in Chapter 3.

[1] R. I. Masel, *Principles of Adsorption and Reaction on Solid Surfaces* (Wiley, New York, 1996).

[2] R. Nibbelke, A. Nievergeld, J. Hoebink, and G. Marin, *Development of a transient kinetic model for the CO oxidation by O_2 over a Pt/Rh/CeO_2/ γ - Al_2O_3 catalyst*, Applied Catalysis B: Environmental **19**, 245 (1998).

[3] P. Hugo, *Stabilität und Zeitverhalten von Durchfluß-Kreislauf-Reaktoren*, Ber. Bunsenges. Phys. Chem. **74**, 121 (1970).

[4] M. Jakubith, *Isotherme Oszillationen bei der CO-Oxidation am Pt-Netz*, Chem. Ing. Tech. **14**, 943 (1970).

[5] G. Ertl, P. R. Norton, and J. Rüstig, *Kinetic oscillations in the platinum-catalysed oxidation of CO*, Phys. Rev. Lett. **49**, 177 (1982).

[6] M. Eiswirth and G. Ertl, *Kinetic oscillations in the catalytic CO oxidation on a Pt(110) surface*, Surf. Sci. **177**, 90 (1986).

[7] M. P. Cox, G. Ertl, R. Imbihl, and J. Rüstig, *Non-equilibrium surface phase transitions during the catalytic oxidation of CO on Pt(100)*, Surf. Sci. **134**, L517 (1983).

[8] M. P. Cox, G. Ertl, and R. Imbihl, *Spatial self-organization of surface structure during an oscillating catalytic reaction*, Phys. Rev. Lett. **54**, 1725 (1985).

[9] K. Krischer, M. Eiswirth, and G. Ertl, *Oscillatory CO oxidation on Pt(110): Modeling of temporal self-organization*, J. Chem. Phys. **96**, 9161 (1992).

[10] M. Bär, N. Gottschalk, M. Eiswirth, and G. Ertl, *Spiral waves in a surface reaction: model calculations*, J. Chem. Phys. **100**, 1202 (1994).

[11] W. Engel, M. E. Kordesch, H. H. Rotermund, S. Kubala, and A. v. Oertzen, *A UHV-compatible photoelectron emission microscope for applications in surface science*, Ultramicroscopy **36**, 148 (1991).

[12] H. H. Rotermund, G. Haas, R. U. Franz, R. M. Tromp, and G. Ertl, *Imaging pattern formation in surface reactions from ultra-high vacuum to atmospheric pressures*, Science **270**, 608 (1995).

[13] H. H. Rotermund, *Imaging pattern formation in surface reactions from ultra-high vacuum up to atmospheric pressures*, Surf. Sci. **386**, 10 (1997).

[14] G. Ertl, in *Handbook of Heterogeneous Catalysis,* G. Ertl, H. Knözinger and J. Weitkamp, Ed. (Wiley-VCH, Weinheim, 1997), pp. 1032.

[15] R. Imbihl, S. Ladas, and G. Ertl, *The CO-induced 1x2-1x1 phase transition of Pt(110) studied by LEED and work function measurements*, Surf. Sci. **206**, L903 (1988).

[16] T. E. Jackman, J. A. Davies, D. P. Jackson, W. N. Unertl, and P. R. Norton, *The Pt(110) phase transition: a study by Rutherford backscattering, nuclear microanalysis, LEED and Thermal Desorption Spectroscopy*, Surf. Sci. **120**, 389 (1982).

[17] G. Doyen and G. Ertl, *Theory of CO chemisorption on transition metal*, Surf. Sci. **43**, 197 (1974).

[18] G. Blyholder, *Molecular orbital view of chemisorbed carbon monoxide*, J. of Chem. Phys. **68**, 2772 (1964).

[19] H. Over and S. Y. Tong, in *Handbook of Surface Science,* W. N. Unertl, Ed. (Elsevier, Amsterdam, 1996), pp. 425.

[20] R. Hoffmann, *A chemical and theoretical way to look at bonding on surfaces*, Rev. Mod. Phys. **60**, 601 (1988).

[21] P. H. Emmett, (Franklin, New York, 1965), pp. 186.

[22] R. K. Sharma, W. A. Brown, and D. A. King, *The adsorption of CO on Pt{110} over the temperature range from 90 to 300 K studied by RAIRS*, Surf. Sci. **414**, 68 (1998).

[23] S. Schwegmann, W. Tappe, and U. Korte, *Quantitative structure analysis of a disordered system: RHEED study of the CO induced (1x2) ->(1x1)structure transition of Pt(110)*, Surf. Sci. **334**, 55 (1995).

[24] P. Hofmann, S. R. Bare, and D. A. King, *Surface phase transitions in CO chemisorption on Pt(110)*, Surf. Sci. **117**, 245 (1982).

[25] A. v. Oertzen, H. H. Rotermund, and S. Nettesheim, *Diffusion of carbon monoxide and oxygen on Pt(110): experiments performed with the PEEM*, Surf. Sci. **311**, 322 (1994).

[26] N. Freyer, M. Kiskinova, G. Pirug, and H. P. Bonzel, *Site-specific core level spectroscopy of CO and NO adsorption on Pt(110) (1x2) and (1x1) surfaces*, Appl. Phys. A **39**, 209 (1986).

[27] N. Freyer, M. Kiskinova, G. Pirug, and H. P. Bonzel, *Oxygen adsorption on Pt(110)-(1x2) and Pt(110)-(1x1)*, Surf. Sci. **166**, 206 (1986).

[28] S. Helveg, J. K. Nørskov, and F. Besenbacher, *Oxygen adsorption on Pt(110)-(1x2): new high-coverage structures*, Surf. Sci. **430**, L533 (1999).

[29] J. Schmidt, C. Stuhlmann, and H. Ibach, *Oxygen adsorption on the Pt(110) (1x2) surface studied with EELS*, Surf. Sci. **284**, 121 (1993).

[30] A. Walker, B. Klotzer, and D. King, *Dynamics and kinetics of oxygen dissociative adsorption on Pt{110}(1x2)*, J. Chem. Phys. **109**, 6879 (1998).

[31] M. Wilf and P. T. Dawson, *The adsorption and desorption of oxygen on the Pt(110) surface; a thermal desorption and LEED/AES study*, Surf. Sci. **65**, 399 (1977).

[32] A. Groß, *Reactions at surfaces studied by ab initio dynamics calculations*, Surf. Sci. Rep. **32**, 293 (1998).

[33] U. Heiz, A. Sanchez, S. Abbet, and W. D. Schneider, *Catalytic oxidation of CO on monodispersed Pt clusters: each atom counts*, J. Am. Chem. Soc. **121**, 3214 (1999).

[34] K. Hauffe, in *Reactivity of Solids,* (Plenum, New York, 1976), pp. 389.

[35] P. A. Cox, *Transition Metal Oxides : An Introduction to Their Electronic Structure and Properties* (Clarendon Pr., Oxford, 1992).

[36] H. P. Bonzel, A. M. Franken, and G. Pirug, *The segregation and oxidation of silicon on Pt(111), or: the question of the "platinum oxide"*, Surf. Sci. **104**, 625 (1981).

[37] M. Berdau, S. Moldenhauer, A. Hammoudeh, J. H. Block, and K. Christmann, *Interaction of oxygen with Pt(210): formation of new oxygen states at higher exposures*, Surf. Sci. **446**, 323–333 (2000).

[38] A. v. Oertzen, A. Mikhailov, H. H. Rotermund, and G. Ertl, *Subsurface oxygen formation on the Pt(110) surface: Experiments and mathematical modelling*, Surf. Sci. **350**, 259 (1996).

[39] J. Falta, R. Imbihl, and M. Henzler, *Spatial pattern formation in a catalytic surface reaction: the facetting of Pt(110) in CO + O_2*, Phys. Rev. Lett. **64**, 1409 (1990).

[40] J.-K. Zuo, Y.-L. He, G.-C. Wang, and T. E. Felter, *High resolution low-energy electron diffraction study of Pt(110)(1 x 2)*, J. Vac. Sci. Technol. A **8**, 2474 (1990).

[41] W. Tappe, U. Korte, and G. Meyer-Ehmsen, *RHEED structure analysis of the oscillatory catalytic CO oxidation at Pt(110) surfaces*, Surf. Sci. **388**, 162 (1997).

[42] R. v. Glan and U. Korte, *The NO-induced (1x2)->(1x1) structural transition of Pt(110): A quantitative RHEED investigation*, Surf. Sci. **375**, 353 (1997).

[43] T. Gritsch, D. Coulman, R. J. Behm, and G. Ertl, *Mechanism of the CO induced 1x2 ->1x1 structural transformation of Pt(110)*, Phys. Rev. Lett. **63**, 1086 (1989).

[44] M. Kantcheva and S. Sayan, *On the mechanism of CO adsorption on a silica-supported ruthenium catalyst*, Catal. Lett. **60**, 27 (1999).

[45] T. Engel and G. Ertl, *A molecular beam investigation of the catalytic oxidation of CO on Pd (111)*, J. Chem. Phys. **69**, 1267 (1978).

[46] A. Alavi, P. Hu, T. Deutsch, P. L. Silvestrelli, and J. Hutter, *CO oxidation on Pt(111): an ab-initio density functional theory study*, Phys. Rew. Lett. **80**, 3650 (1998).

[47] K. Bleakley and P. Hu, *A density functional theory study of the interaction between CO and O on a Pt surface.*, J. Am. Chem. Soc. **121**, 7644 (1999).

[48] C. Stampfl, H. Kreuzer, S. Payne, and M. Scheffler, *Challenges in predictive calculations of processes at surfaces: surface thermodynamics and catalytic reactions*, Appl. Phys. A **69**, 471 (1999).

[49] S. Nettesheim, A. v. Oertzen, H. H. Rotermund, and G. Ertl, *Reaction-diffusion patterns in the catalytic CO oxidation on Pt(110). Front propagation and spiral waves*, J. Chem. Phys. **98**, 9977 (1993).

[50] V. P. Zhdanov, *Simulation of kinetic oscillations in catalytic reactions accompanied by adsorbate-induced surface restructuring*, Surf. Sci. **426**, 345 (1999).

[51] H. Risken, *The Fokker-Planck Equation* (Springer, Berlin, Heidelberg, 1989).

[52] M. Gerhardt, H. Schuster, and J. J. Tyson, *A cellular automaton model of excitable media*, Physica D **46**, 392 (1990).

[53] M. Bär, M. Falcke, C. Zülicke, H. Engel, M. Eiswirth, and G. Ertl, *Reaction fronts and pulses in the CO oxidation on Pt: theoretical analysis*, Surf. Sci. **269/270**, 471 (1992).

[54] Y. Kuramoto, *Chemical Oscillations, Waves and Turbulence* (Springer, Berlin, 1984).

[55] L. Onsager, Phys. Rev. **38**, 2256 (1931).